Discordance of the Areas of Peak Wall Shear Stress and Tissue Stress in Coronary Artery Plaques as Revealed by Fluid-Structure Interaction Finite Element Analysis

A Case Study

Tatsuya ASANUMA,[1] MEnv, Yasutomi HIGASHIKUNI,[2] MD, Hiroshi YAMASHITA,[2] MD, Ryozo NAGAI,[2,3] MD, Toshiaki HISADA,[1] PhD, *and* Seiryo SUGIURA,[1] MD

SUMMARY

Simulation studies have been performed in attempts to elucidate the significance of shear and tissue stresses in the progression and rupture of coronary artery plaques, but few studies have analyzed both stresses simultaneously. We analyzed the distributions of shear stress and tissue stress in a model of coronary artery plaque based on intravascular ultrasound data by fluid-structure interaction finite element analysis under physiological pressure and flow. As shown in previous studies, the region of peak shear stress was observed at the proximal side of the plaque where flow velocity was high but its value was at most 10 Pa. On the other hand, 1000–10,000 times greater tissue stress was located in the stenotic region but the location of peak tissue stress was different from that of shear stress. We also found that stenting not only stabilizes the stented segment but also reduces the stress in the adjacent region. Fluid-structure interaction analysis revealed discordance in the distribution of shear and tissue stresses. These two stresses exert distinct influences on the coronary plaque, rupture of which may occur where tissue stress exceeds the plaque strength, which is weakened by pathological processes triggered by shear stress. (Int Heart J 2013; 54: 54-58)

Key words: Coronary plaque, Finite element method

The pathophysiology of coronary artery disease is significantly influenced by the local interplay between mechanical stimuli and biological responses.[1)] Cyclically changing intramural pressure and flow in the coronary arteries and the motion of vessels accompanying the heart beat (tethering) create a highly heterogeneous mechanical environment, which could account for the spatial distribution of atherosclerotic lesions. Major components of mechanical stimulus (stress) include wall shear stress applied by the blood flowing to the arterial endothelium, tensile stress due to the distension of the vessel wall, and the bending and stretching of the wall resulting from the tethering effect of surrounding tissues. Experimental studies have shown that cyclic changes in shear stress modulate the permeability and proliferation of endothelial cells.[2,3)] Shear stress is also involved in the accumulation of lipids, and inflammatory cell recruitment and adhesion, thus playing a pivotal role in the progression and vulnerability of atherosclerotic plaques.[4-6)] On the other hand, cyclic stretch also induces such changes to initiate the atherosclerotic process[7,8)] and, more importantly, the high stress generated during tissue deformation can be a direct cause of plaque rupture.[9,10)] However, extrapolation of these findings to clinical cases is hampered by the difficulty in performing *in vivo* measurements of these mechanical parameters.

To circumvent this problem, researchers have utilized the numerical simulation to analyze stress and strain distributions in coronary vessels. In these studies, either 2D (transverse section) or 3D morphologies of coronary arteries were modeled as idealized or realistic models based on angiogram, computed tomography (CT), or intravascular ultrasound (IVUS) images[9-16)] to demonstrate that clinically observed sites of prediction for atherosclerotic plaque formation and rupture show close correlations with the distributions of these mechanical parameters. To date, however, most of these studies have evaluated either only wall shear stress (computational fluid dynamics: CFD) ignoring the deformation of vessel wall or only tissue stress (structural analysis) without considering the blood flow because of the complexity and difficulty of the numerical analysis. Coupled analysis of flow dynamics and structural deformation called fluid-structure interaction (FSI) is eagerly needed not only for the accurate estimation of these stresses but because of the close interplay between them in the pathophysi-

From the [1] Department of Human and Engineered Environmental Studies, Graduate School of Frontier Sciences, The University of Tokyo, Chiba, [2] Department of Cardiovascular Medicine, Graduate School of Medicine, The University of Tokyo, Tokyo, [3] Jichi Medical University, Tochigi, Japan.

This work was supported by the Japan Society for the Promotion of Science through its Funding Program for World-Leading Innovative R&D on Science and Technology (FIRST Program).

Address for correspondence: Seiryo Sugiura, MD, Graduate School of Frontier Sciences, The University of Tokyo, 5-1-5 Kashiwanoha, Kashiwa-shi, Chiba 277-8563, Japan.

Received for publication September 24, 2012.
Revised and accepted November 2, 2012.

ology of atherosclerotic plaques.[17] For instance, both wall shear stress and tissue stress are implicated in plaque rupture but their relative contributions should be clarified by FSI analysis in a realistic coronary artery model.

Very recently, the need for and importance of FSI for the analysis of vascular diseases has been recognized, however, the number of applications is still limited, especially to the carotid artery.[17,18] Therefore, in this study, we applied FSI analysis to both blood flow and wall deformation in a realistic coronary artery model based on IVUS images. The obtained distribution of wall shear stress and tissue stress differed significantly, thereby demonstrating the need and importance of FSI analysis.

Case Report

Among the patients who have undergone coronary interventions at The University of Tokyo Hospital, one case, an 83 year old male, was selected and his clinical data were obtained with informed consent. A lesion located in the straight segment was selected. This study protocol was approved by the Institutional Review Board of The University of Tokyo.

IVUS data acquisition and mesh generation: Images of the proximal segment of the left anterior descending artery were recorded by IVUS (Atlantis SR Pro, 2.8F, 40 MHz, Boston Scientific Corporaton/SCIMED, Maple Grove, MN, USA). The transducer was withdrawn using an auto-pullback system at 0.5 mm/s. In this study, 21 slices covering the lesion were used for model construction. The intervals between slices were 0.25 mm or 0.5 mm depending on the morphology of the vessel. Each slice was segmented manually to delineate the lumen, plaque component, and vessel out-boundary. Stent struts were not explicitly segmented but the finite elements cut across by the stent were assigned a hard tissue property. From these data, we constructed the 3-D vessel geometry of the coronary artery segment and blood in the lumen as a finite element model consisting of 20,065 tetrahedral elements using the mesh generation software written in our laboratory.

Fluid-structure interaction analysis: The details of fluid-structure interaction analysis developed in our laboratory have been described elsewhere.[19] Blood flow was assumed to be Newtonian and incompressible. The strain energy function describing the isotropic tissue material properties of the plaque and vessel wall were adopted from the literature[17] with some modifications in parameter values. Governing equations for fluid (blood) and structure (vessel wall) parts were solved simultaneously using the strong coupling method. We prescribed physiological boundary conditions in the following two steps. First, we increased the luminal pressure to 12 kPa (≒ 90 mmHg) to distend the vessel wall. Next, cyclically changing flow (1 Hz, velocity range 0.06 - 0.3 m/second) was applied to the proximal end and a similar pattern of cyclically changing pressure (70 - 110 mmHg) was prescribed at the distal end following the method of Yang, *et al.*[17] All the finite element computer programs were written in our laboratory.

Patient specific model: Figure 1 shows the IVUS images (A) and constructed finite element model (B) of the stented segment of the proximal left anterior descending artery. In this segment, two Xience V stents (Abbott Vascular, IL) (2.75 × 23 mm to the proximal site and 2.5 × 28 mm to the distal site, indicated by the thick double headed arrows) were implanted. To save computational cost, only part of the stented segments was included.

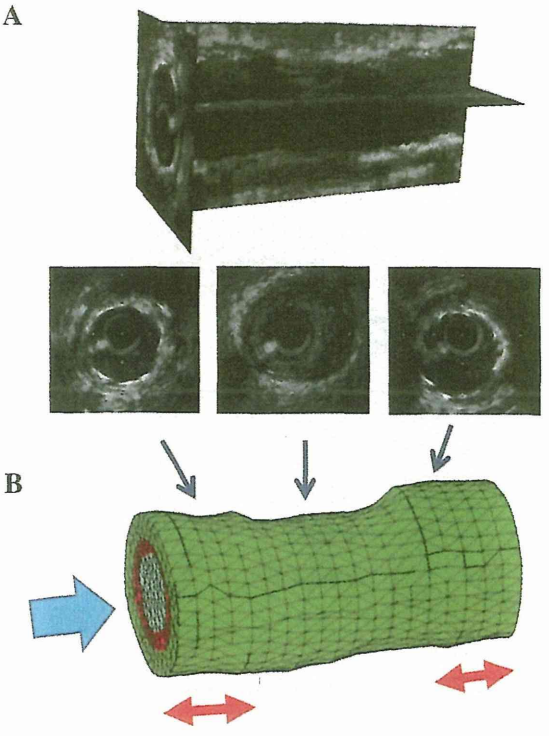

Figure 1. A: Reconstructed IVUS images of the coronary artery segment modeled in this study. Cross-sections of stented segments and the plaque lesion are shown below. **B:** Finite element model. Blood flow was applied from the left end (blue arrow) and pressure was prescribed at the right end. Double headed arrows indicate the stented segments.

Pressure and flow distribution: Figure 2A shows the distribution of flow velocity. Although we applied physiological flow with uniform distribution at the inlet (Figure 2B), the stenosis in the middle disturbed the distribution and a vortex was observed after the stenotic region (Figure 2A inset). Figure 2C shows the pressure prescribed at the outlet. Because the stenosis was not severe in this case, the pressure difference between the inlet and outlet was as small as 0.9 mmHg.

Wall shear stress and tissue stress: Figure 3A shows the distribution of wall shear stress. Similar to earlier studies, high wall shear stress was observed at the stenotic site, where flow velocity was high (Figure 2A). The peak wall shear stress was detected on the proximal side of the plaque but its value was at most 10 Pa. Tissue stress was analyzed in two ways. First, we plotted the intraplaque distribution of von Mises stress (Appendix; Figure 3B), which reflects the shear stress energy often used to determine the yield criterion of steel. Similar to the wall shear stress, a region of high stress was observed at the stenotic region, but its distribution was broad covering the whole circumference. Finally, principal (tensile) stress was plotted as shown in Figure 3C. The maximum tensile stress was found in the stenotic region, but its location was shifted upstream from the location of the maximum wall shear stress. In the thick-walled cylinder structure-like arteries, the direction of tensile stress should be aligned in the circumferential direc-

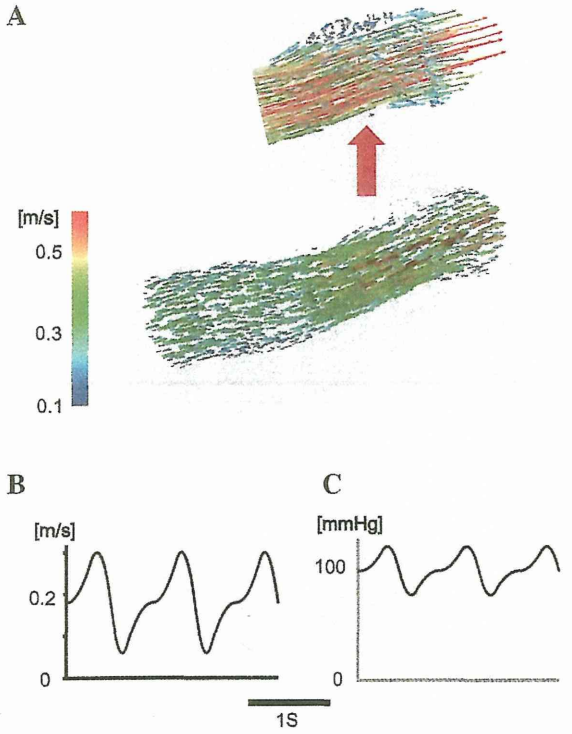

Figure 2. **A:** Flow velocity distribution. The inset shows the magnification of the poststenotic region where a vortex is observed. **B:** Flow velocity applied to the inlet (left). **C:** Prescribed pressure at the outlet (right).

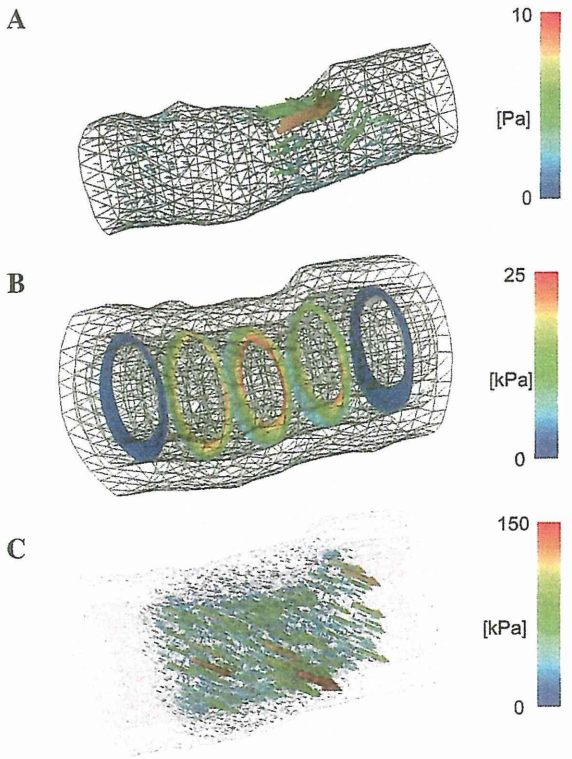

Figure 3. **A:** Distribution of wall shear stress. The mesh indicates the luminal surface. **B:** Distribution of von Mises stress in the plaque. **C:** Distribution of principal (maximum tensile) stress.

tion; however, in this case, it was tilted by 45 degrees or so. The simulation also demonstrated that the tissue stress is 1000 (von Mises stress) to 10,000 (principal stress) times greater than wall stress.

Stenting may reduce the tissue stress: We simulated a case in which stents were not implanted in the arterial segment by changing the material property in the stented region. Figure 4 compares the deformation of the luminal surfaces (upper row) and von Mises stress between the stented (A) and nonstented (B) cases during the cardiac cycle. It is noteworthy that not only the stented region at both ends but also the nonstented middle region was stabilized by stenting as evidenced by the overlapping of black (diastolic) and red (systolic) meshes in the top left panel. As a result, without stents, the von Mises stress increased throughout the segment (Figure 4B).

Discussion

In this study, we analyzed both wall shear stress and tissue stress in a patient specific model of a coronary artery using fluid-structure interaction finite element analysis. Although only one case was analyzed, the results provided us with a unique opportunity to consider the implications of these mechanical factors in the pathophysiology of coronary artery disease.

Fluid-structure interaction analysis: Recent developments in imaging modalities and their applications in clinical cardiology have enabled us to construct a realistic model of coronary arteries. CFD analyses performed on a 3D model of epicardial coronary vessels based on bi-plane angiograms or CT data revealed high wall shear stress on the stenotic site and vortex formation in the distal segment.[16,20,21] A detailed model of the vascular segment based on IVUS images also suggested causal relations between the high wall shear stress and plaque development or rupture.[13,14] In these studies, however, vessel walls were treated as a rigid tube thus totally ignoring their deforma-

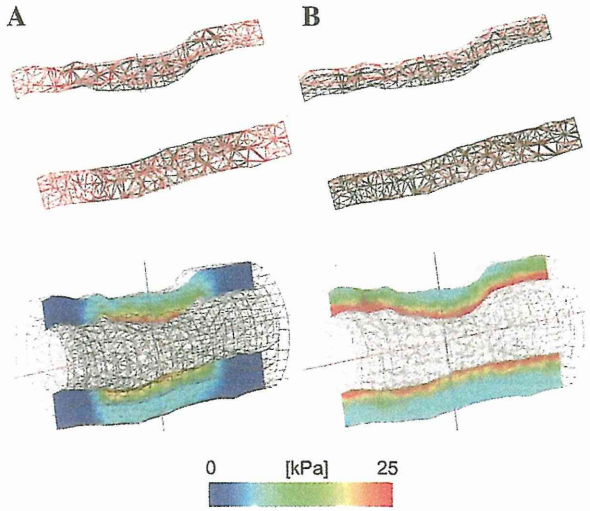

Figure 4. Deformation of the vessel (upper panels) and von Mises stress (bottom panels) in the stented (**A**) and nonstented (**B**) cases during the cardiac cycle. In the upper panels, the black meshes represent the diastolic shape of the vessel and the red meshes represent the systolic shape.

tion due to the pulsatile luminal pressure and cardiac contraction. Another salient feature of IVUS imaging is its capability for tissue characterization. IVUS-based 2D or 3D models of coronary arteries segmented into fibrous plaque, lipid core, and vascular tissue have been used in the stress and/or strain analyses of vascular tissue subjected to intravascular pressure.[9,10,15] Basic and clinical studies have successfully identified the regions of high stress in plaque, which are implicated in the progression and rupture of plaques. However, in these studies, only structural deformation was considered and blood flow was ignored. Considering the fact that wall deformation and blood flow in the vessel are tightly coupled, simulation studies simultaneously solving these two phenomena are needed for an understanding of the pathophysiology of coronary artery disease. To date, however, few studies have analyzed FSI in coronary arteries owing to the difficulty of such an analysis. In one such study, Yang, *et al* modeled a short segment of the right coronary artery of a patient to report the distributions of tissue stress and flow velocity as a preliminary study, but no clinical implications were presented.[17]

Wall shear stress versus tissue stress: One of the main purposes of simulation studies is to identify the mechanical factor responsible for the plaque progression and/or rupture. Whereas the significance of wall shear stress in the progression of atherosclerotic plaque has been widely studied, its causal role in plaque rupture is controversial. Recently, Fukumoto, *et al* reported that high wall shear stress was concentrated in the assumed rupture site in clinical cases.[14] However, as shown in their study as well as ours, the absolute value of wall shear stress is too small to be a direct cause. On the other hand, even in a limited number of cases, Ohayon, *et al* demonstrated coincidence of the area of circumferential tensile peak stress with the location of plaque rupture triggered by balloon angioplasty.[9] Again, we note that both studies calculated only wall shear stress or tissue stress.

Although plaque rupture was not documented, we could evaluate both wall shear stress and tissue stress in a clinical case. Similar to earlier studies, high wall shear stress and tissue stress were concentrated in the plaque region but their distributions differed slightly. This raises the question of which location is at potential risk of rupture? We hypothesize that 1) wall shear stress stimulates various biological processes to make the plaque vulnerable, and 2) plaque rupture takes place where tissue stress exceeds the plaque strength (Figure 5A). The location of plaque rupture does not necessarily coincide with the peak of wall shear stress or tissue stress (Figure 5B). Further studies including many clinical cases with detailed information on the morphology and properties of plaque tissue are needed to validate these hypotheses and make the prediction of rupture risk a possibility in the near future.

Finally, we also found that implantation of stents stabilizes and reduces the deformation of adjacent segments. This finding may help optimize strategies for coronary intervention.

Limitations: Although this was a preliminary study, the use of a single case to construct our model limits the clinical implications of our findings. Follow-up analyses on many cases should be performed in the future. On the technical side, improvement of the modeling method is needed. Firstly, finer segmentation of IVUS images coupled with the proper assignment of a material property to each tissue should be attempted for more accurate evaluation and risk estimation. Second, although reported to be negligible in an earlier study,[17] the bending motion of the vessels by cardiac contraction must be included to simulate the heart under various conditions. Finally, although high performance computing is required, a large scale model including the whole coronary artery tree coupled with a beating heart model will surely help us understand the complex interplay among the tissue deformation and blood flow in the pathogenesis of coronary artery disease.

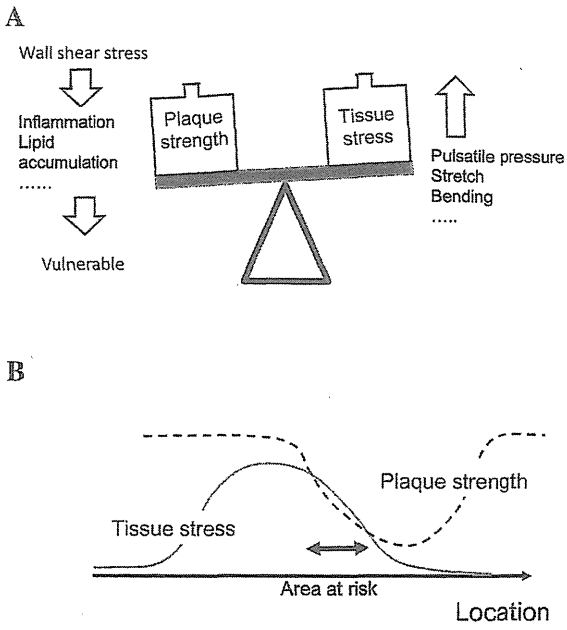

Figure 5. **A:** Conflicting factors causing plaque rupture **B:** Conceptual diagram showing the area at risk.

Appendix

von Mises stress was calculated by the following equation:

$$\sigma_M = \sqrt{\frac{1}{2}\{(S_{11}-S_{22})^2+(S_{22}-S_{33})^2+(S_{33}-S_{11})^2+3(S_{12}^2+S_{21}^2+S_{23}^2+S_{12}^2+S_{31}^2+S_{32}^2)\}}$$

References

1. Vanepps JS, Vorp DA. Mechano-pathobiology of atherogenesis: a review. J Surg Res 2007; 142: 202-17. (Review)
2. Himburg HA, Grzybowski DM, Hazel AL, LaMack JA, Li XM, Friedman MH. Spatial comparison between wall shear stress measures and porcine arterial endothelial permeability. Am J Physiol Heart Circ Physiol 2004; 286: H1916-22.
3. White CR, Haidekker M, Bao X, Frangos JA. Temporal gradients in shear, but not spatial gradients, stimulate endothelial cell proliferation. Circulation 2001; 103: 2508-13.
4. Chatzizisis YS, Coskun AU, Jonas M, Edelman ER, Feldman CL, Stone PH. Role of endothelial shear stress in the natural history of coronary atherosclerosis and vascular remodeling: molecular, cellular, and vascular behavior. J Am Coll Cardiol 2007; 49: 2379-93. (Review)
5. Helderman F, Segers D, de Crom R, *et al*. Effect of shear stress on vascular inflammation and plaque development. Curr Opin in Lipidol 2007; 18: 527-33. (Review)
6. Ridger V, Krams R, Carpi A, Evans PC. Hemodynamic parameters regulating vascular inflammation and atherosclerosis: a brief up-

date. Biomed Pharmacother 2008; 62: 536-40. (Review)
7. Howard AB, Alexander RW, Nerem RM, Griendling KK, Taylor WR. Cyclic strain induces an oxidative stress in endothelial cells. Am J Physiol 1997; 272: C421-7.
8. Wang DL, Wung BS, Shyy YJ, *et al.* Mechanical strain induces monocyte chemotactic protein-1 gene expression in endothelial cells. Effects of mechanical strain on monocyte adhesion to endothelial cells. Circ Res 1995; 77: 294-302.
9. Ohayon J, Teppaz P, Finet G, Rioufol G. In-vivo prediction of human coronary plaque rupture location using intravascular ultrasound and the finite element method. Coron Artery Dis 2001; 12: 655-63.
10. Imoto K, Hiro T, Fujii T, *et al.* Longitudinal structural determinants of atherosclerotic plaque vulnerability: a computational analysis of stress distribution using vessel models and three-dimensional intravascular ultrasound imaging. J Am Coll Cardiol 2005; 46: 1507-15.
11. Baldewsing RA, de Korte CL, Schaar JA, Mastik F, van der Steen AF. Finite element modeling and intravascular ultrasound elastography of vulnerable plaques: parameter variation. Ultrasonics 2004; 42: 723-9.
12. Versluis A, Bank AJ, Douglas WH. Fatigue and plaque rupture in myocardial infarction. J Biomech 2006; 39: 339-47.
13. Wahle A, Lopez JJ, Olszewski ME, *et al.* Plaque development, vessel curvature, and wall shear stress in coronary arteries assessed by X-ray angiography and intravascular ultrasound. Med Image Anal 2006; 10: 615-31.
14. Fukumoto Y, Hiro T, Fujii T, *et al.* Localized elevation of shear stress is related to coronary plaque rupture: a 3-dimensional intravascular ultrasound study with in-vivo color mapping of shear stress distribution. J Am Coll Cardiol 2008; 51: 645-50.
15. Liang Y, Zhu H, Gehrig T, Friedman MH. Measurement of the transverse strain tensor in the coronary arterial wall from clinical intravascular ultrasound images. J Biomech 2008; 41: 2906-11.
16. De Santis G, Mortier P, De Beule M, Segers P, Verdonck P, Verhegghe B. Patient-specific computational fluid dynamics: structured mesh generation from coronary angiography. Med Biol Eng Comput 2010; 48: 371-80.
17. Yang C, Bach RG, Zheng J, *et al.* In vivo IVUS-based 3-D fluid-structure interaction models with cyclic bending and anisotropic vessel properties for human atherosclerotic coronary plaque mechanical analysis. IEEE Trans Biomed Eng 2009; 56: 2420-8.
18. Teng Z, Canton G, Yuan C, *et al.* 3D critical plaque wall stress is a better predictor of carotid plaque rupture sites than flow shear stress: An in vivo MRI-based 3D FSI study. J Biomech Eng 2010; 132: 031007.
19. Zhang Q, Hisada T. Analysis of fluid-structure interaction problems with structural buckling and large domain changes by ALE finite element method. Comput Methods Appl Mech Engrg 2001; 190: 6341-57.
20. Katritsis DG, Theodorakakos A, Pantos I, *et al.* Vortex formation and recirculation zones in left anterior descending artery stenoses: computational fluid dynamics analysis. Phys Med Biol 2010; 55: 1395-411.
21. Chaichana T, Sun Z, Jewkes J. Computation of hemodynamics in the left coronary artery with variable angulations. Biomech 2011; 44: 1869-78.